

Diffusion Dynamics of Metal Ions Uptake at the Carboxylated-Epichlorohydrin Red Onion Skin Extract Resin – Aqueous Interface

Millicent U. Ibezim-Ezeani*, Onyewuchi Akaranta**

**(Department of Department of Pure and Industrial Chemistry, University of Port Harcourt, P.M.B. 5323, Choba, Port Harcourt, Nigeria.*

** *(Department of Department of Pure and Industrial Chemistry, University of Port Harcourt, P.M.B. 5323, Choba, Port Harcourt, Nigeria.*

ABSTRACT

Investigation into the diffusion dynamics of Mn^{2+} , Fe^{2+} and Pb^{2+} ions uptake from aqueous solution by chemically modified red onion skin extract was carried out. The polyhydroxylic extract of red onion skin was utilized in the synthesis of carboxylated-epichlorohydrin red onion skin extract resin (CERR). The fourier transform infrared spectra of red onion skin extract and CERR exhibited variations in bond interactions which was ascribed to the structural modification of the extract to yield CERR. Predictions of the mechanism of diffusion dynamics were carried out by applying the data resolved from the fractional attainment of equilibrium at varied times into the Vermeulen diffusion models within the temperature range of 29 to 70°C. The predominance of film diffusion mechanism was established from the smaller values of its diffusion coefficients as compared to those of particle diffusion. The film diffusion coefficient values were lowest at 29°C, indicating the most probable temperature condition for optimum exchange result with the CERR. Deductions from utilizing the Arrhenius type temperature dependence equation gave negative values of activation energy (-7.223 kJ/mol for Mn^{2+} , -6.898 kJ/mol for Fe^{2+} and -13.957 kJ/mol for Pb^{2+} ions); which suggests that increase in temperature from 29 to 70°C, lowered the rate of the exchange reaction.

Keywords: Diffusion dynamics, ion exchange resin, metal ions, red onion skin, Vermeulen diffusion models

I. INTRODUCTION

Diffusion is the spontaneous migration of particulate matter due to spatial gradient in concentration. The direction of the random motion of the diffusing species is down its gradient in a bid to adjust the imbalance in particle density. Thus, for a particular medium, the rate at which substances diffuse in or out of the system and its surrounding is dependent on the variability of parameters like concentration, pressure, temperature and density with change in distance and time. The dominance of diffusion and its principles have gained impetus in many technologies associated with separation, purification, redox reaction, ionic conductivity, solubility, catalysis, recrystallization, water softening, substitution, demineralization, corrosion and so on.

This paper presents the diffusion dynamics of Fe^{2+} , Mn^{2+} and Pb^{2+} ions exchange at the CERR – aqueous interface. Ion exchange is based on the principle of diffusion and is the stoichiometric chemical reaction in which the interchange of equivalent ions at the phase boundary is reversible [1]. Diffusion dynamics of ion exchange describes the gradient in chemical kinetics of the interchange of equivalent ions between the exchanging and exchangeable species at a given condition with time

until the process attains the state of no net transfer of mass and energy at the interface.

In a given system, the steps that determine the diffusion dynamics of ion exchange process are the:

- (i) Migration of exchanging ions through the bulk solution to the boundary film surrounding the surface of the resin particles.
- (ii) Migration of exchanging ions from the boundary through the layer of film to the resin particles surface (film diffusion).
- (iii) Migration of exchanging ions from the resin surface to the intra-particle active sites (particle diffusion).
- (iv) Interchange of equivalent ions between the exchanging and the exchangeable species at the active internal surfaces of the resin particles (ion exchange).
- (v) Outward migration of exchanged ions from the particle interior to the surface of the resin particles (particle diffusion).
- (vi) Outward migration of exchanged ions from the resin surface to the boundary film surrounding the particles (film diffusion).
- (vii) Migration of exchanged ions from the boundary film into the bulk solution.

The steps (vii), (vi) and (v) are the reverse of steps (i), (ii) and (iii) respectively, suggesting mutual action of dominance between the film and particle diffusion mechanisms within a particular period in the exchange process. Earlier research reports emphasized that film diffusion could be ascribed the rate controlling mechanism, if uneven distribution of substance exist in the liquid film layer, coupled with prevalence of similar ionic composition throughout the exchanger. Conversely, if the concentration of ions in the exchanger is not equally proportioned, but uniformly spread within the film layer, then the condition is suggestive of particle diffusion as the rate limiting mechanism [2].

The chief interest of this investigation is to deduce the mechanism underlying the diffusion dynamics of metal ion removal with the formulated resin. The findings will form the basis for planning and modifying the process to required scale in order to achieve greater efficiency in the retrieval of metal ions from metal contaminated effluents.

II. EXPERIMENTAL

2.1 Collection and Preparation of Sample

Bulbs of red onion were sourced from the fruit garden market in Port Harcourt, Nigeria for the purpose of this investigation. The papery outer layer was peeled from the onion bulb, washed with deionised water and air dried for 3 days. The air dried skin was ground with an electric milling machine, sieved to particle size of 150 μm and preserved in corked plastic container at 29 $^{\circ}\text{C}$.

2.2 Extraction Procedure

The extraction of 2940 g of 150 μm size red onion skin was performed using soxhlet extractor with acetone (BDH) as the extracting solvent. The solvent-extract mixture was transferred to rotor evaporator, and the extracted sample recovered by expelling acetone.

2.3 Spectroscopic Studies

The formulation of CERR was through the reaction of the extract with epichlorohydrin (Sigma Aldrich) and 4-hydroxybenzoic acid (Sigma Aldrich) [3, 4]. The characteristic functional groups present in the molecular structure of the extract and CERR samples were resolved using the Fourier Transform Infrared spectrometer (prestige 21 shimadzu) with potassium bromide pressed disc method in the frequency range of 4000 – 400 cm^{-1} .

2.4 Preparation of Standard Solutions

The dissolution of 3.0785 g of $\text{MnSO}_4 \cdot \text{H}_2\text{O}$, 4.973 g of $\text{FeSO}_4 \cdot 7\text{H}_2\text{O}$ and 1.59 g of $\text{Pb}(\text{NO}_3)_2$ in distilled deionised water to obtain 1000 mg/l metal ion stock solutions were each prepared in 1litre volumetric flask. All reagents used were of

analytical grade. Necessary dilution of the respective stock solutions was done to obtain 50 mg/l concentration of the metal ion solution.

2.5 Ion Exchange Study

The batch exchange experiments were carried out by placing 1g of CERR and 50 cm^3 of 50 mg/l metal (Mn^{2+} / Fe^{2+} / Pb^{2+}) ion solution into several conical flasks, then corked and shaken at the rate of 120 oscillations / min for different agitation times of 2 to 60 mins at 29 $^{\circ}\text{C}$. The resultant suspensions were centrifuged and filtered through glass wool. The clear filtrate was analysed using the Atomic Absorption Spectrophotometer (Perkin Elmer, Analyst 200) and the concentration of metal ion in the liquid phase was ascertained. Systematic batch experiments were conducted as described above for the metal ions at temperatures of 40, 50, 60 and 70 $^{\circ}\text{C}$.

III. RESULTS AND DISCUSSION

3.1 Spectroscopic Analysis

The Fourier Transform Infrared of the extract and CERR were recorded at the percentage transmittance in the frequency range of 4000 – 400 cm^{-1} and depicted in Figs. 1 and 2 respectively. The functional group assignments for the absorption bands and their possible interpretation [5,6] are presented in Table 1.

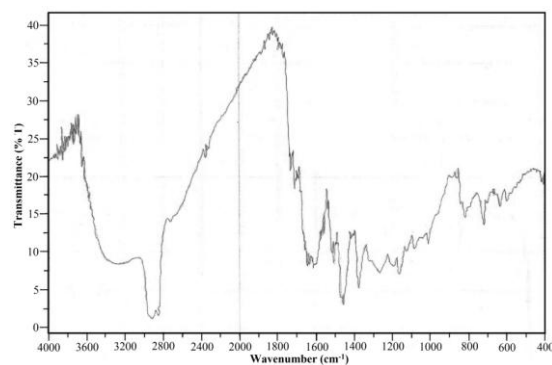


Fig. 1: Infrared Spectrum of Red Onion Skin Extract

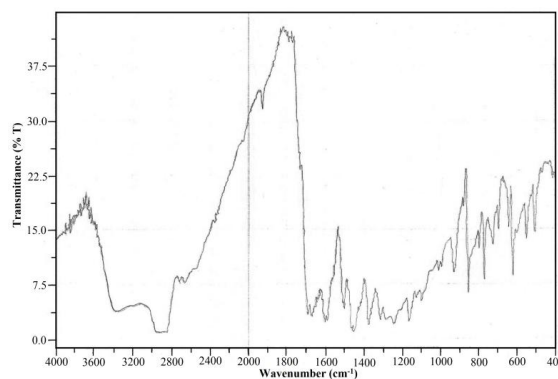


Fig. 2: Infrared Spectrum of CERR

Spectra analyses display some differences in the absorption bands, apparently as a result of changes in the surface properties, emanating from the modification of the extract to yield CERR. The infrared spectrum of CERR (Fig. 2) showed a prominent peak at 1930 cm⁻¹, representing weak overtone and combination of aromatic C-H stretching bands which is characteristic of the substitution pattern of the ring. An obvious peak at 930 cm⁻¹ in the CERR spectrum reflects the existence of intermolecular forces within the ring structure, arising from asymmetrical ring stretching in which the C-C bond is stretching during contraction of the C-O bond. Another pronounced peak at 495 cm⁻¹ corresponds to C-C bending vibrations, due to bond interaction effects within the CERR molecular structure. The percentage transmittance for the infrared spectrum of the extract is relatively higher than that of CERR, indicating the influence of substitution on the structural arrangement of the CERR molecule. Further examination reveals that this difference could be related to the variation in their dipole moments [7], evidenced by changes in vibration, rotation, stretching or bending of bonds at specific frequencies of the energy in the infrared range studied. This also confirms the conversion of the extract to a new compound (CERR). The Synthesis of 4-(2,3-Epoxypropoxy) benzoic acid and proposed coupling of CERR are presented in Figs. 3 and 4 respectively.

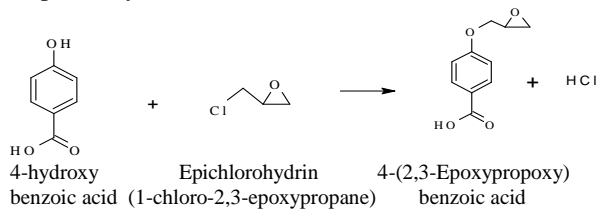


Fig. 3: Synthesis of 4-(2,3-Epoxypropoxy) benzoic acid

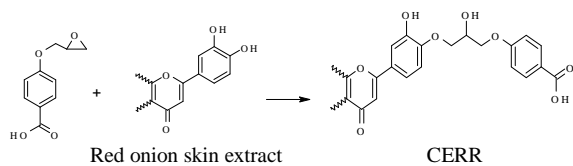


Fig. 4: Proposed Coupling of CERR

3.2 Diffusion Dynamics Study

Investigation into the values of the particle and film diffusion coefficients was performed by applying the time dependent data to Vermeulen diffusion models in Eqs. (1) and (2) respectively [8]:

$$-\ln(1 - \alpha^2) = t \left(\frac{D_p \pi^2}{r_p^2} \right) \quad (1)$$

$$-\ln(1 - \alpha) = t \left(\frac{3D_f C_o}{r_p \delta C_e} \right) \quad (2)$$

$$\alpha = \frac{C_o - C_t}{C_o - C_e} \quad (3)$$

where α (fractional attainment of equilibrium) is the metal ion exchanged at a particular time divided by that at equilibrium (Eq. 3) [9]; C_o , C_t and C_e are the metal ion concentration initially, at time, t (min) and equilibrium (mg/l) respectively; D_p and D_f are diffusion coefficients (m²/min) in the ion exchanger and film respectively, r_p is the particle radius (m) and δ is the film thickness (m). The film thickness, δ can be deduced from the fringing effect in Fig. 2 using Eq. (4) [10]:

$$\delta = \frac{1}{2n} \times \frac{N}{(v_1 - v_2)} \quad (4)$$

where n is the refractive index of sample (1.362), N is the number of fringes within a given spectral region (4 in this case), v_1 and v_2 are the start and end points in the spectrum (1375 and 1165 cm⁻¹ respectively). The plots of $-\ln(1 - \alpha^2)$ and $-\ln(1 - \alpha)$ versus time at different temperatures are presented in Figs. 5 to 10.

The plots in Figs. 5 to 10 are straight lined and their R² values are listed in Table 2. The slope of the plots were deduced and represented as S_p and S_f for the particle and film diffusion respectively. Following Eqs. (1) and (2), S_p and S_f could be expressed as Eqs. (5) and (6) respectively:

$$S_p = \frac{D_p \pi^2}{r_p^2} \quad (5)$$

$$S_f = \frac{3D_f C_o}{r_p \delta C_e} \quad (6)$$

The D_f and D_p are then made the subject of the formula in Eqs. (7) and (8) respectively. The values of D_f and D_p computed at temperatures of 29 to 70°C are presented in Table 2 for the metal ions.

$$D_p = \frac{S_p r_p^2}{\pi^2} \quad (7)$$

$$D_f = \frac{S_f \delta C_e r_p}{3C_o} \quad (8)$$

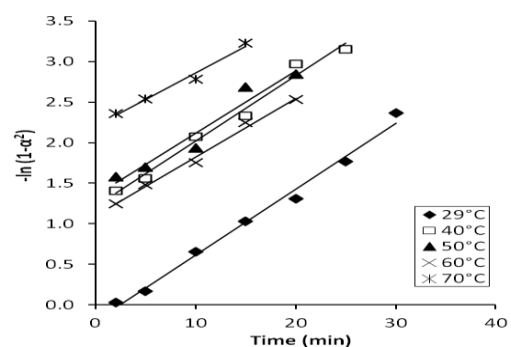


Fig. 5: Vermeulen particle diffusion model isotherms for Mn²⁺ ion

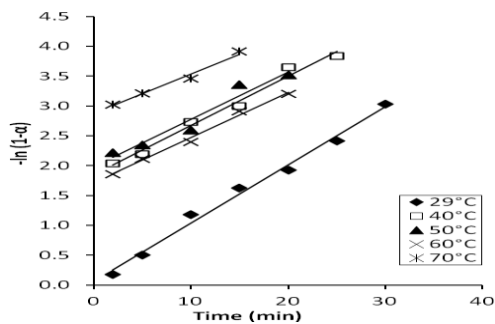


Fig. 6: Vermeulen film diffusion model isotherms for Mn^{2+} ion

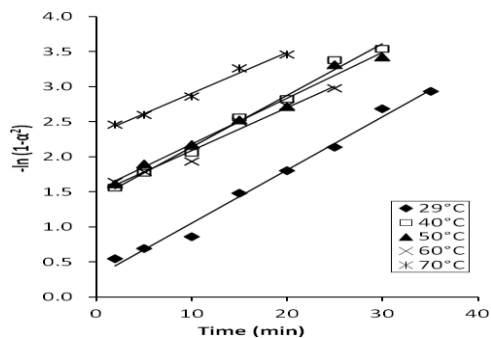


Fig. 7: Vermeulen particle diffusion model isotherms for Fe^{2+} ion

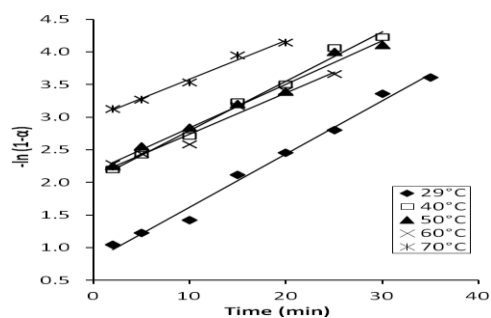


Fig. 8: Vermeulen film diffusion model isotherms for Fe^{2+} ion

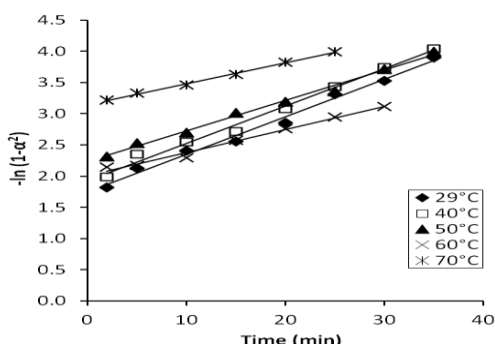


Fig. 9: Vermeulen particle diffusion model isotherms for Pb^{2+} ion

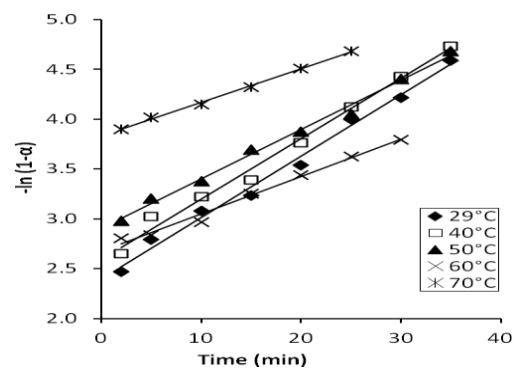


Fig. 10: Vermeulen film diffusion model isotherms for Pb^{2+} ion

Data analyses show that the values of the film diffusion coefficient range from $4.551 \times 10^{-11} - 1.229 \times 10^{-10} \text{ m}^2/\text{min}$ ($7.86 \times 10^{-7} - 4.58 \times 10^{-6} \text{ cm}^2/\text{s}$) for Mn^{2+} , $6.566 \times 10^{-11} - 1.189 \times 10^{-10} \text{ m}^2/\text{min}$ ($1.62 - 5.61 \times 10^{-6} \text{ cm}^2/\text{s}$) for Fe^{2+} and $7.227 \times 10^{-11} - 7.868 \times 10^{-11} \text{ m}^2/\text{min}$ ($3.17 - 11.53 \times 10^{-6} \text{ cm}^2/\text{s}$) for Pb^{2+} ions; while that of particle diffusion is from $1.852 \times 10^{-10} - 1.483 \times 10^{-10} \text{ m}^2/\text{min}$ ($4.63 - 5.72 \times 10^{-6} \text{ cm}^2/\text{s}$) for Mn^{2+} , $1.736 \times 10^{-10} - 1.328 \times 10^{-10} \text{ m}^2/\text{min}$ ($4.93 - 6.44 \times 10^{-6} \text{ cm}^2/\text{s}$) for Fe^{2+} and $1.373 \times 10^{-10} - 7.607 \times 10^{-11} \text{ m}^2/\text{min}$ ($6.23 \times 10^{-6} - 1.13 \times 10^{-5} \text{ cm}^2/\text{s}$) for Pb^{2+} ions. These values infer that the limiting mechanism for metal ions uptake rate is film diffusion, since the values of D_f are lower than those of D_p . Research on the rate of ammonium uptake by natural zeolite and transcarpathian mordenite reported $0.7 - 3.6 \times 10^{-12} \text{ m}^2/\text{s}$ and $1.26 - 9.73 \times 10^{-12} \text{ m}^2/\text{s}$ range of coefficient values for particle diffusion and film diffusion respectively. The research team remarked that the ion exchange reaction was dominated by the model of particle diffusion and ascribed their findings to the influence of structural feature of the mordenite mineral fraction on the process [8]. Vinod and Anirudhan studied tannic acid sorption on zirconium pillared clay; and reported values within $10^{-9} \text{ cm}^2/\text{s}$ and $10^{-7} \text{ cm}^2/\text{s}$ for D_p and D_f respectively. They hinted that the process is not purely film diffusion controlled but involves particle diffusion in the latter stages [11]. The diffusivity values deduced in the biosorption of Cr (VI) ion by *Aeromonas caviae* decreased with increase in temperature from 20 to 60 °C, apparently due to the modification of surface geometry of the biomass at elevated temperatures [12].

Also, the values of coefficient of determination (R^2) within the temperature range (Table 2) tested reflects a little difference between that of film and particle diffusion models, suggesting a complementary relationship between their mechanisms. However, the higher R^2 values for the film diffusion mechanism in all cases, is an evidence of its superior influence over that of particle diffusion on the exchange process.

The relationship that correlates the time dependence of the fractional attainment of equilibrium, α is given in Eq. (9) [13]. The plots of $\ln(1 - \alpha)$ against time are depicted in Figures 11, 12 and 13 for Mn^{2+} , Fe^{2+} and Pb^{2+} respectively.

$$\ln(1 - \alpha) = -kt \quad (9)$$

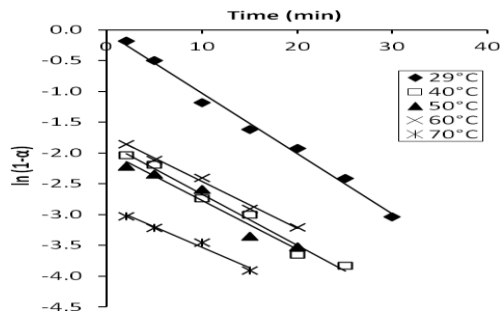


Fig. 11: Plot of $\ln(1-\alpha)$ against time for Mn^{2+} ion

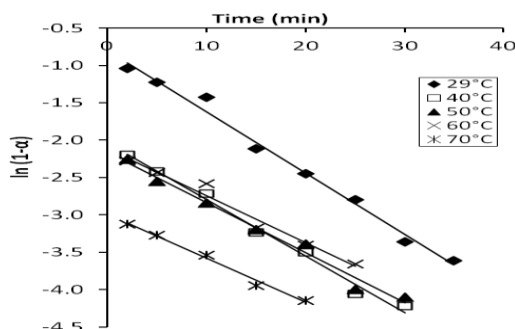


Fig. 12: Plot of $\ln(1-\alpha)$ against time for Fe^{2+} ion

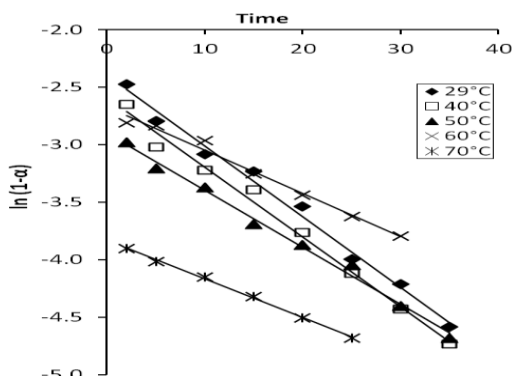


Fig. 13: Plot of $\ln(1-\alpha)$ against time for Pb^{2+} ion

The reaction rate constants (k) at different temperatures were extrapolated from the slope of the straight line plots of $\ln(1 - \alpha)$ against time and the values presented in Table 2. The values of k decreased in the order: $29 > 40 > 50 > 60 > 70$ °C, indicating that the rate of reaction is highest at 29 °C within the temperature range tested.

The temperature dependence of ion exchange rates was demonstrated by the linear behavior of the plot of $\ln k$ versus $1/T$ (Fig. 14) using the Arrhenius expression [14,15] in Eq. (10):

$$\ln k = \ln A - \frac{E_a}{RT} \quad (10)$$

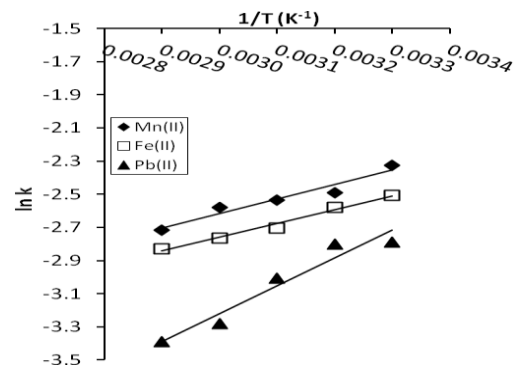


Fig. 14: Arrhenius plots for the metal ions

where A , E_a , R and T are the pre-exponential factor, activation energy, gas constant and temperature respectively. The values of E_a and A were computed from the slope and intercept of the plots, and presented in Table 3. The E_a values represent the lowest amount of kinetic energy which is sufficient for effective interaction between the exchanging and exchangeable species in the systematic uptake of the metal ions.

Table 3: Kinetic parameters for the exchange process with CERR

Metal ion	Linear equation	A [min ⁻¹]	E _a [kJ/mol]
Mn^{2+}	$y = 868.8x - 5.222$	5.395×10^{-3}	-7.223
Fe^{2+}	$y = 829.7x - 5.248$	5.257×10^{-3}	-6.898
Pb^{2+}	$y = 1678.0x - 8.258$	2.592×10^{-4}	-13.957

If the value of E_a is positive, it signifies that the rate constant is strongly temperature dependent; If E_a is zero, its rate is not dependent on temperature and if E_a is negative, it indicates that the rate is inversely proportional to temperature [16]. The negative values of E_a deduced in this study, therefore suggest that the exchange rate is most favored at 29 °C within the experimental temperatures. The pre-exponential factor incorporates the frequency of molecular collision and geometric requirement for the orientation of the colliding molecules of the reactants [17]. The calculated values of A are in the order: $Mn^{2+} > Fe^{2+} > Pb^{2+}$, which is in line with that of their ionic radii. This indicates that the smaller the metal ionic size, the more enhanced its diffusion to the active site with time, and the higher the probability of its proper spatial positioning to produce useful molecular impact at the moment of contact.

IV. CONCLUSION

The extract of red onion skin (a biodegradable agro waste) has been applied in the synthesis of cation exchange resin for the uptake of Mn^{2+} , Fe^{2+} and Pb^{2+} ions from aqueous medium. The infrared spectroscopic examination of the red onion skin extract and CERR in the frequency range of

4000 to 400 cm^{-1} revealed some differences in their absorption bands, possibly due to the successful modification of extract to yield a new compound (CERR). The Vermeulen diffusion equations were used to study the diffusion dynamics of the exchange process at temperatures of 29 to 70 °C. The film diffusion exhibited smaller values of diffusion coefficients as compared to those of particle

diffusion, and was therefore considered as the rate controlling mechanism. Application of the rate constants evaluated at temperatures of 29, 40, 50, 60 and 70 °C to the Arrhenius equation, resulted in E_a with negative values indicating that the exchange process is more favored at 29 °C.

ACKNOWLEDGEMENTS

Special thanks to Prof. Raphael Ngochindo (Department of Pure and Industrial Chemistry, University of Port Harcourt, Rivers State, Nigeria) for supporting this work with useful suggestions. We also appreciate Miss Kate Iwunor (FUGRO Ltd, Eleme, Rivers State, Nigeria) for the spectrophotometric analyses.

REFERENCES

- [1]. M. U. Ibezim-Ezeani, F. A. Okoye, O. Akaranta, *Int. J. Water Res. Environ. Eng.*, 4 (6) (2012) 192-200.
- [2]. A. Jignasa, R. Thakkar, C. Uma, *J. Chem. Sci.*, 118 (2) (2006) 185-189.
- [3]. M. U. Ibezim-Ezeani, A. F. Okon, *Res. J. Chem. Sci.*, 6 (9) (2016) 49-54.
- [4]. M. U. Ibezim-Ezeani, O. Akaranta, *Int. J. ChemTech Res.*, 9 (9) (2016) 550-562.
- [5]. B. A. Uzoukwu, *Basic Analytical Chemistry*, millennium ed., Paragraphics, Port Harcourt, Nigeria, 2009.
- [6]. R. M. Silverstein, G. C. Bassier, T. C. Morrill, *Spectrometric Identification of Organic Compounds*, 5th ed., John Wiley and Sons, Inc., USA, 1991.
- [7]. C. L. Beh, T. G. Chuah, M. N. Nourouzi, T. S. Y. Choong, *E-J. Chemistry*, 9 (4) (2012) 2557- 2564.
- [8]. M. Sprynskyy, M. Lebedynets, R. Zbytniewski, J. Namieśnik, B. Buszewski, *Separation Purification Technol.*, 46 (2005) 155-160.
- [9]. M. Sekar, V. Sakthi, S. Rengaraji, *J. Colloid Interface Sci.*, 279 (2004) 307-313.
- [10]. Pike Technologies Spectroscopic Creativity, Calculating the thickness of free – standing Films by FTIR, Application Note – 0502, www.piketech.com (accessed 12th June, 2016).
- [11]. V. P. Vinod, T. S. Anirudhan, *J. Chem. Technol. Biotechnol.*, 77 (2001) 92-101.
- [12]. M. X. Loukidou, D. K. Thodoris, A. L. Zouboulis, K. A. Matis, *Ind. Eng. Chem. Res.*, 43 (2004) 1748-1755.
- [13]. G. Karthikeyan, K. Anbalagan, N. M. Andal, *J. Chem. Sci.*, 116 (2) (2004) 119-127.
- [14]. M. U. Ibezim-Ezeani, A. C. I. Anusiem, *Int. J. Phys. Sci.*, 5 (9) (2010) 62-67.
- [15]. D. Kaušpėdienė, E. Kazlauskienė, A. Selskienė, *Ion Exchange Letters*, 3 (2010) 19-24.
- [16]. P. W. Atkins, *Physical Chemistry*, 6th ed., Oxford University Press, New York, 1998.
- [17]. A. C. I. Anusiem, *Principles of General Chemistry*, revised ed., Versatile Publishers, Owerri, Nigeria, 2000.

Table 1: Infrared absorption bands and their functional group assignments

Absorption bands [cm^{-1}]		Functional group assignments	Possible interpretation
Extract	Resin		
3400 - 3250	3400 - 3300	O-H	Broad band attributed to the O-H stretching of intermolecular hydrogen bonded hydroxyl groups Absorption bands indicate the presence of C-H stretching Weak combination and overtone bands of aromatic C-H stretching appear in the 2000 – 1650 cm^{-1} region
2950 - 2825	2970 - 2850, 2660	C-H	
	1930	C-H	
1725, 1715, 1660	1690	C=O	Absorption peaks in the C=O stretching region of carboxylic acids and ketones
1590, 1505, 1460	1600, 1500, 1460	C=C	Skeletal vibrations involving C=C stretching within the ring, absorb in the 1600 – 1585 and 1500 – 1400 cm^{-1} region
1370	1375	C-O	Mulls, pellets or melts of phenols absorb at 1390 – 1330 and 1260 -1180 cm^{-1} bands, apparently resulting from interaction between O-H bending

1270, 1160, 1020	1320,1290, 1245, 1165,1100	C-O	and C-O stretching. Also O-H in – plane bending vibration occurs in the general region of 1420 – 1330 cm ⁻¹ These wave numbers are in the C-O stretching region (1300 – 1050 cm ⁻¹) of alcohols, carboxylic acids and ethers
	930	C-C	Band appearing in the 950 – 810 cm ⁻¹ region is attributed to asymmetrical ring stretching in which the C-C bond is stretching during contraction of the C-O bond
820, 720	860, 765, 720,700	C-H	The most characteristic absorption of polynuclear aromatics results from C-H out-of-plane ring bending in the 900 – 675 cm ⁻¹ region
635, 605	650, 620, 550	C-Br	Brominated compounds absorb in the 690 – 515 cm ⁻¹ region
	495	C-C	The C-C bending vibrations occur at frequencies below 500 cm ⁻¹ region

Table 2: Coefficients of determination (R²) and parameters for the diffusion dynamics

Metal Ion	Temp [°C]	k [min ⁻¹]	Film diffusion [-ln(1- α)]			Particle diffusion [-ln(1- α ²)]		
			R ²	Regression Equation	D _f [m ² min ⁻¹]	R ²	Regression Equation	D _p [m ² min ⁻¹]
Mn ²⁺	29	0.0978	0.9909	y = 0.0978x + 0.0555	4.551 x 10 ⁻¹¹	0.9902	y = 0.0813x - 0.1959	1.852 x 10 ⁻¹⁰
	40	0.0828	0.9832	y = 0.0828x + 1.8457	5.999 x 10 ⁻¹¹	0.9831	y = 0.0802x + 1.2198	1.827 x 10 ⁻¹⁰
	50	0.0794	0.9454	y = 0.0794x + 1.9817	7.486 x 10 ⁻¹¹	0.9444	y = 0.0769x + 1.3493	1.752 x 10 ⁻¹⁰
	60	0.0758	0.9920	y = 0.0758x + 1.7095	1.062 x 10 ⁻¹⁰	0.9918	y = 0.0725x + 1.0987	1.651 x 10 ⁻¹⁰
	70	0.0662	0.9806	y = 0.0662x + 2.8728	1.229 x 10 ⁻¹⁰	0.9801	y = 0.0651x + 2.2060	1.483 x 10 ⁻¹⁰
Fe ²⁺	29	0.0817	0.9897	y = 0.0817x + 0.8017	6.566 x 10 ⁻¹¹	0.9885	y = 0.0762x + 0.2887	1.736 x 10 ⁻¹⁰
	40	0.0757	0.9901	y = 0.0757x + 2.0362	7.170 x 10 ⁻¹¹	0.9900	y = 0.0739x + 1.3970	1.683 x 10 ⁻¹⁰
	50	0.0670	0.9837	y = 0.0670x + 2.1661	8.259 x 10 ⁻¹¹	0.9836	y = 0.0655x + 1.5222	1.492 x 10 ⁻¹⁰
	60	0.0631	0.9938	y = 0.0631x + 2.1124	1.008 x 10 ⁻¹⁰	0.9937	y = 0.0613x + 1.4735	1.396 x 10 ⁻¹⁰
	70	0.0591	0.9896	y = 0.0591x + 2.9892	1.189 x 10 ⁻¹⁰	0.9895	y = 0.0583x + 2.3193	1.328 x 10 ⁻¹⁰
Pb ²⁺	29	0.0614	0.9903	y = 0.0614x + 2.3993	7.227 x 10 ⁻¹¹	0.9902	y = 0.0603x + 1.7440	1.373 x 10 ⁻¹⁰
	40	0.0607	0.9902	y = 0.0607x + 2.5890	8.169 x 10 ⁻¹¹	0.9901	y = 0.0598x + 1.9272	1.362 x 10 ⁻¹⁰
	50	0.0495	0.9927	y = 0.0495x + 2.9030	8.036 x 10 ⁻¹¹	0.9925	y = 0.0489x + 2.2338	1.114 x 10 ⁻¹⁰
	60	0.0376	0.9875	y = 0.0376x + 2.6707	7.271 x 10 ⁻¹¹	0.9874	y = 0.0368x + 2.0100	8.382 x 10 ⁻¹¹
	70	0.0337	0.9980	y = 0.0337x + 3.8301	7.868 x 10 ⁻¹¹	0.9979	y = 0.0334x + 3.1473	7.607 x 10 ⁻¹¹